

## Fluoride adsorption properties of three modified forms of activated alumina in drinking water

Ying Duan, Chenchen Wang, Xuede Li and Wei Xu

### ABSTRACT

The study describes the removal of fluoride from drinking water using activated alumina (AA). AA was modified with H<sub>2</sub>SO<sub>4</sub>, FeCl<sub>3</sub> and a combination of the two to enhance fluoride adsorption. The AA adsorbents were characterized using Brunauer–Emmett–Teller surface area analysis and X-ray fluorescence. The maximum adsorption capacity of H<sub>2</sub>SO<sub>4</sub>- and FeCl<sub>3</sub>-modified AA adsorbents was 4.98 mg/g, which is 3.4 times higher compared with that of normal AA. The results showed that the surface area of AA increased when modified with H<sub>2</sub>SO<sub>4</sub>. AA modified with FeCl<sub>3</sub> enhanced fluoride adsorption ability through ion-exchange between chlorine ions and fluoride ions. The fluoride adsorption properties of AA modified with both H<sub>2</sub>SO<sub>4</sub> and FeCl<sub>3</sub> were consistent with the Langmuir model. The fluoride adsorption kinetics of the adsorbents were well described by the pseudo-second-order kinetic model.

**Key words** | adsorption, fluoride, modified activated alumina

Ying Duan  
Chenchen Wang  
Xuede Li  
Wei Xu (corresponding author)  
School of Resource and Environment,  
Anhui Agricultural University,  
Hefei 230036,  
China  
E-mail: dy\_0725@163.com

### INTRODUCTION

Fluorine is an important trace element for humans and animals. Fluorine has both beneficial and harmful effects on the human body. Within the permissible limit, beneficial effects of fluoride for the human body include the calcification of dental enamel and maintenance of healthy bones. The excessive intake of fluoride can cause dental and skeletal forms of fluorosis, and its accumulation over a long period can also lead to changes in the DNA structure (Sehn 2008). The World Health Organization has set a guideline value of 1.5 mg/L as the maximum permissible level of fluoride for drinking water (WHO 2006). Worldwide, there are about 200 million people with great health risks due to high fluoride content in their available drinking water (Sivasankar *et al.* 2011). In China, the safe limit of fluoride concentration in drinking water is below 1.0 mg/L. In China, over 60 million people in over 27 provinces and municipalities are suffering from fluorosis (Zhang *et al.* 2012). Hence, it is necessary to use an effective and safe technique for the removal of excess fluoride from water.

Currently, various defluoridation techniques have been developed to decrease the fluoride content to under the

permissible limits. The techniques available for defluoridation include adsorption (Ghorai & Pant 2004; Daifullah *et al.* 2007), ion exchange (Vaaramaa & Lehto 2003), chemical precipitation (Meenakshi & Maheshwari 2006), and electro dialysis (Ghosh *et al.* 2008). Among these technologies, electro dialysis and ion exchange processes are not commonly used due to their high installation and maintenance costs, while the major disadvantage of chemical precipitation is generation of unwanted chemicals and waste disposal issues (Maliyekkal *et al.* 2008; Mohapatra *et al.* 2009; Camacho *et al.* 2010). The adsorption process is considered a widely accepted technique because of its cost-effectiveness, economics, flexibility, simplicity of design, and ease of operation and maintenance for treating drinking water systems, especially for small communities (Ayooob & Gupta 2007).

A wide range of adsorbents have been used for fluoride removal, such as activated alumina (AA) (Tripathy *et al.* 2006), iron and iron oxide (Bang *et al.* 2005), clays (Meenakshi *et al.* 2008), and zeolites (Onyango *et al.* 2004). Among these adsorbents, AA has been extensively studied and used for defluoridation of drinking water because it is easily available

and inexpensive. Moreover, AA is also appropriate for large-scale defluoridation due to its chemical/physical properties and bulk availability (Ghorai & Pant 2005). However, the low adsorption capacity and slow rate of adsorption limit its use for treating a large quantity of water. To overcome this limit, much research has been conducted to modify AA in order to improve its adsorption capacity. For example, Maliyekkal *et al.* (2008) modified AA with magnesium oxide, and Tripathy & Raichur (2008) coated AA with manganese dioxide. Both studies reported that the adsorption capacity and adsorption rate had increased significantly with the modifications. However, these two modification methods are not appropriate for defluorination of drinking water because the AA should be calcined at high temperature.

To improve the fluoride adsorption properties of AA using some safe, simple and feasible modification methods, we studied AA modifications with three salts,  $\text{FeCl}_3$ ,  $\text{Fe}_2(\text{SO}_4)_3$ ,  $\text{Al}_2(\text{SO}_4)_3$ , and  $\text{H}_2\text{SO}_4$ . Comparing the adsorption capacity of these modified AAs, the AA modified with both  $\text{H}_2\text{SO}_4$  and  $\text{FeCl}_3$  had the best adsorption capability. In this study, AA was modified with  $\text{H}_2\text{SO}_4$  and  $\text{FeCl}_3$ . To achieve the optimal condition of modification with  $\text{H}_2\text{SO}_4$  and  $\text{FeCl}_3$ , we conducted a series of studies including adsorption kinetics, adsorption isotherms and surface characteristics to study the adsorption properties and mechanism.

## METHODS

### Materials

The AA was purchased from a local plant (Gongyi Chemical Reagent Plant, Gongyi, Henan, China) and then crushed and sieved to a particle size range of 0.25–0.425 mm. All chemicals used in this study were analytical grade. Stock fluoride solution was prepared by dissolving an appropriate quantity of sodium fluoride in deionized water.

### Preparation of different modified AAs

#### $\text{H}_2\text{SO}_4$ -modified activated alumina ( $\text{H}_2\text{SO}_4$ -MAA)

The AA was soaked in 0.02 M  $\text{H}_2\text{SO}_4$  solution for 2 hours with a solid/solution ratio of 1:3. The solution was washed

with deionized water until around pH 7, and dried at 110 °C for 2 hours.

#### $\text{FeCl}_3$ -modified activated alumina ( $\text{FeCl}_3$ -MAA)

The AA was soaked in 0.1%  $\text{FeCl}_3$  solution for 6 hours with a solid/solution ratio of 1:5. The solution was washed with deionized water until around pH 7, and dried at 110 °C for 2 hours.

#### $\text{H}_2\text{SO}_4$ with $\text{FeCl}_3$ -modified activated alumina ( $\text{H}_2\text{SO}_4$ + $\text{FeCl}_3$ -MAA)

The AA was soaked in 0.01 M  $\text{H}_2\text{SO}_4$  solution for 2 hours with a solid/solution ratio of 1:3. Then the product was washed with deionized water until pH 7, and dried at 110 °C for 2 hours. Then,  $\text{H}_2\text{SO}_4$ -MAA was soaked in 0.1%  $\text{FeCl}_3$  solution for 3 hours with a solid/solution ratio of 1:10. The solution was washed with deionized water until around pH 7, and dried at 110 °C for 2 hours.

### Characterization of adsorbents

The test samples were washed with deionized water and dried at 110 °C. The textural properties of MAA and AA, such as surface area, pore volume, and pore size, were measured with a Brunauer–Emmett–Teller (BET) surface area analyzer (Tristar II 3020 M, Micromeritics, USA) with nitrogen ( $\text{N}_2$ ) at 77 K. After alumina was ground and tableted, element analysis of alumina was carried out by X-ray fluorescence (XRF) (XRF-1800, SHIMADZU, Japan). The ion concentrations of water with adsorption of different adsorbents were analyzed by inductively coupled plasma mass spectrometry (ICP-MS) (ICP-6300, Thermo Electron, USA).

### Batch adsorption experiments

Batch experiments were conducted in 250 mL flasks containing 100 mL fluoride solution. After adding 0.4 g adsorbents to the fluoride solution, the flasks were kept in a shaker with thermostatic control at 200 rpm and 25 °C for a specified contact time.

The amount of fluoride adsorbed was calculated using the following equation:

$$q_e = \frac{(C_0 - C_e) * V_0}{m} \quad (1)$$

where  $q_e$  is the adsorption capacity of the adsorbents at equilibrium (mg/g);  $C_0$ ,  $C_e$  are initial and equilibrium concentration of fluoride (mg/L), respectively;  $V_0$  is the volume of the fluoride solution (L) and  $m$  is the mass of adsorbents used in the experiments (g).

## Methods of analysis

The fluoride concentration in the treated water samples was analyzed by a selective electrode method using an ion meter coupled with a fluoride ion selective electrode. Total ionic strength adjustment buffer (TISAB) was used to maintain the pH and background ion concentration. Experiments were repeated twice for better accuracy and blank experiments were conducted throughout the studies.

## RESULTS AND DISCUSSION

### Adsorption rate curves

Figures 1(a) and 1(b) show the adsorption rates of three samples of MAA and AA at different concentrations of fluoride. The adsorption rates of the three samples of MAA and AA at various initial fluoride concentrations were similar (Figure 1). The adsorption capacity increased quickly during the first 3 hours and a slow increase was observed after 3 hours until equilibrium was reached. The equilibrium time of AA was 5–8 hours. The equilibrium time of MAA was 8 hours at low initial fluoride and 12 hours at high initial fluoride. The remaining fluoride concentration in water adsorbed by MAA was lower than that by AA, especially at low initial fluoride concentration (5 mg/L). When the initial fluoride concentration was 5 mg/L, the remaining fluoride concentration in water defluorinated by MAA was lower than the standards for drinking water quality in China. The defluorination rate of  $H_2SO_4 + FeCl_3$ -MAA

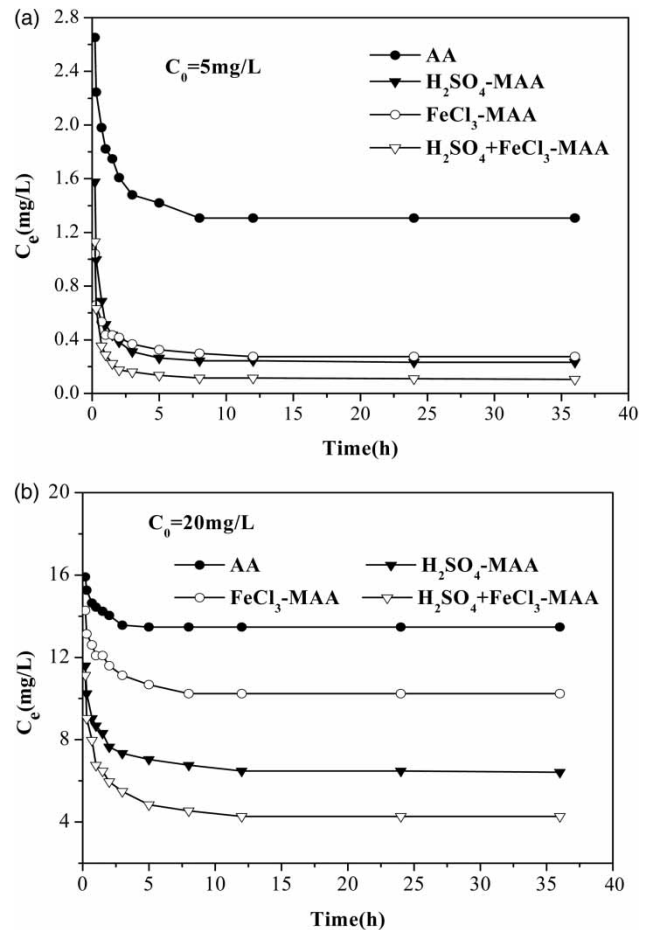


**Figure 1** | Adsorption rate of fluoride removal by three MAAs and AA at various initial concentrations of fluoride (adsorbent dose = 4 g/L, time = 0.2–36 hours).

reached 97% at low initial fluoride concentration, and 75% at high fluoride concentration.

### Adsorption kinetics

The reaction-based models, which include pseudo-first-order and pseudo-second-order models, were applied to fit experimental data (Ma et al. 2007). Fitting results of kinetics data by two models are shown in Table 1. The pseudo-first-order kinetic rate equation (Equation (2)) and the linear form of pseudo-second-order kinetic rate equation (Equation (3)) are represented as follows:

$$\log(q_e - q_t) = \log q_e - \frac{k_1}{2.303} t \quad (2)$$

**Table 1** | Fitted parameters of the first- and second-order equations

Adsorbents	Initial fluoride concentration (mg/L)	Pseudo-first-order			Pseudo-second-order		
		$q_e$ (mg/g)	$k_1$ (1/h)	$R^2$	$q_e$ (mg/g)	$k_2$ (g/(mg·h))	$R^2$
AA	5	0.93	0.11	0.6056	0.93	7.45	0.999
	20	1.64	0.12	0.4037	1.64	4.47	0.998
H <sub>2</sub> SO <sub>4</sub> -MAA	5	1.2	0.08	0.5226	1.2	13.59	0.999
	20	3.45	0.13	0.8930	3.45	1.22	0.998
FeCl <sub>3</sub> -MAA	5	1.19	0.07	0.5896	1.18	18.37	0.999
	20	2.45	0.14	0.6425	2.46	1.79	0.998
H <sub>2</sub> SO <sub>4</sub> + FeCl <sub>3</sub> -MAA	5	1.24	0.06	0.4218	1.23	41.78	0.999
	20	3.91	0.17	0.6268	3.92	2.58	0.999

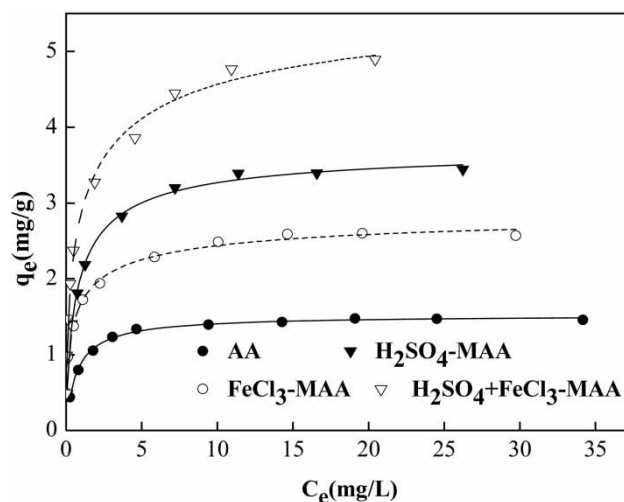
$$\frac{t}{q_t} = \frac{1}{k_2 q_e^2} + \frac{1}{q_e} t \quad (3)$$

where  $k_1$  is the pseudo-first-order rate constant of adsorption (1/h);  $k_2$  is the pseudo-second-order rate constant of adsorption ((g/(mg·h));  $q_e$  and  $q_t$  are the amounts of fluoride adsorbed at equilibrium (mg/g) and at time  $t$  (h), respectively.

As indicated in Table 1, the  $R^2$  values of the pseudo-second-order model ( $>0.99$ ) were much higher than those of the pseudo-first-order model ( $<0.90$ ), and the calculated adsorption capacity of the pseudo-second-order model was also close to the values in the experiments. These indicated the applicability of the pseudo-second-order model for adsorption kinetics of the four adsorbents in this study. For the four adsorbents tested in this study, the pseudo-second-order rate constant  $k_2$  was low, indicating that the rate of the fluoride adsorption process was fast. We observed that the rate constant decreased with the initial fluoride concentrations.

### Adsorption isotherms

In Figure 2, we show the fluoride adsorption equilibrium data obtained on the four adsorbents at initial fluoride concentrations ranging from 2 to 40 mg/L. Among the four adsorbents, H<sub>2</sub>SO<sub>4</sub> + FeCl<sub>3</sub>-MAA showed the highest adsorption capacity. The equilibrium data were fitted using Langmuir and Freundlich models (Tavakoli & Ghasemi 2010). The values of isotherm constants and parameters are given in Table 2.

**Figure 2** | Adsorption isotherms of fluoride on three samples of MAA and AA (fitting by Langmuir isotherm).

In all cases, the coefficients ( $R^2 \geq 0.9971$ ) for the Langmuir plots were always higher than those obtained from the Freundlich model, thus the experimental data were better fitted using the Langmuir model. Table 2 shows that experimental data are in good agreement with the Langmuir isotherm. The rate constant  $b$  of H<sub>2</sub>SO<sub>4</sub> + FeCl<sub>3</sub>-MAA was 1.73, indicating that the rate of the fluoride adsorption process on H<sub>2</sub>SO<sub>4</sub> + FeCl<sub>3</sub>-MAA was high. According to the result fitted by the Langmuir model, the maximum adsorption capacity of H<sub>2</sub>SO<sub>4</sub> + FeCl<sub>3</sub>-MAA (4.98 mg/g) was 3.4 times the adsorption capacity of AA. These indicated that the adsorption ability of H<sub>2</sub>SO<sub>4</sub> + FeCl<sub>3</sub>-MAA was good.

The essential characteristics of the Langmuir isotherm,  $R_L$  was used to test whether the adsorption is favorable or

**Table 2** | Langmuir and Freundlich adsorption model parameters

Adsorbents	Langmuir model			Freundlich model		
	$q_{\max}$ (mg/g)	$b$ (L/mg)	$R^2$	$n$	$K_f$	$R^2$
AA	1.47	1.75	0.9984	4.6104	0.7988	0.8233
H <sub>2</sub> SO <sub>4</sub> -MAA	3.51	1.6	0.9996	3.2744	1.6315	0.9008
FeCl <sub>3</sub> -MAA	2.63	2.14	0.9993	4.3066	1.4207	0.9143
H <sub>2</sub> SO <sub>4</sub> + FeCl <sub>3</sub> -MAA	4.98	1.73	0.9971	3.1766	2.3719	0.8975

not.  $R_L$  can be calculated by the following equation:

$$R_L = \frac{1}{1 + bC_0} \quad (4)$$

where  $C_0$  is the initial solute concentration (mg/L) and  $b$  is the Langmuir adsorption equilibrium constant (L/mg).

If,  $R_L > 1$  is the unfavorable adsorption;  $0 < R_L < 1$  is the favorable adsorption;  $R_L = 1$  is the linear adsorption;  $R_L = 0$  is the irreversible adsorption. The initial fluoride concentration was from 2 to 40 mg/L, and the corresponding values of  $R_L$  were between 0.01 and 0.23, which indicated that the adsorption of fluoride by H<sub>2</sub>SO<sub>4</sub> + FeCl<sub>3</sub>-MAA was the favorable adsorption.

### Characterization of adsorbents

Fluoride adsorption capacity of adsorbents mainly depended on the crystalline form and surface properties (Bhatnagar et al. 2011). The results of BET are shown in Table 3.

As shown in Table 3, the surface area of H<sub>2</sub>SO<sub>4</sub>-MAA increased by 10.5% over that of AA. A possible cause was that impurities in pores of AA were dissolved by H<sub>2</sub>SO<sub>4</sub>. The number of adsorption sites on AA had increased. The surface area of FeCl<sub>3</sub>-MAA and H<sub>2</sub>SO<sub>4</sub> + FeCl<sub>3</sub>-MAA was a little smaller than AA. These results indicated that the increase of adsorption capacity of FeCl<sub>3</sub>-MAA and H<sub>2</sub>SO<sub>4</sub> + FeCl<sub>3</sub>-MAA was not due to the increase of surface area.

In order to compare the element contents of AA and H<sub>2</sub>SO<sub>4</sub> + FeCl<sub>3</sub>-MAA before and after fluoride adsorption,

**Table 3** | BET results of adsorbents

Adsorbents	BET surface area (m <sup>2</sup> /g)	Pore volume (cm <sup>3</sup> /g)	Pore diameter (nm)
AA	117.4	0.41	13.94
H <sub>2</sub> SO <sub>4</sub> -MAA	129.8	0.42	12.84
FeCl <sub>3</sub> -MAA	112.9	0.40	13.98
H <sub>2</sub> SO <sub>4</sub> + FeCl <sub>3</sub> - MAA	115.9	0.40	13.86

the adsorbents were analyzed by XRF. The results are shown in Table 4.

As shown in Table 4, the amount of Cl and S increased after modification with FeCl<sub>3</sub>. After fluoride adsorption, the content of Cl and S on H<sub>2</sub>SO<sub>4</sub> + FeCl<sub>3</sub>-MAA was significantly reduced. This indicated there may be an ion-exchange reaction between Cl<sup>-</sup> or SO<sub>4</sub><sup>2-</sup> and F<sup>-</sup> during the fluoride adsorption process. In order to determine which ion exchanged with F<sup>-</sup>, the ion concentrations of different adsorbents in water after adsorption were analyzed by ICP-MS. The results are shown in Table 5.

As shown in Table 5, the concentration of Cl<sup>-</sup> and SO<sub>4</sub><sup>2-</sup> ions in water increased after defluoridation by AA and H<sub>2</sub>SO<sub>4</sub> + FeCl<sub>3</sub>-MAA, especially SO<sub>4</sub><sup>2-</sup> ions. The concentration of Cl<sup>-</sup> and SO<sub>4</sub><sup>2-</sup> ions in water after defluoridation by H<sub>2</sub>SO<sub>4</sub> + FeCl<sub>3</sub>-MAA was higher than that by AA. These results indicated that Cl<sup>-</sup> and SO<sub>4</sub><sup>2-</sup> ions were loaded on the surface of AA when modified with H<sub>2</sub>SO<sub>4</sub>

**Table 4** | Element contents of different adsorbents (%)

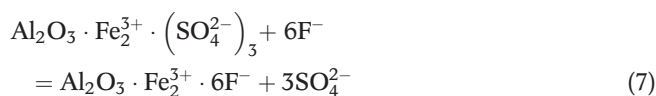
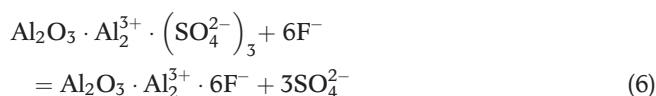
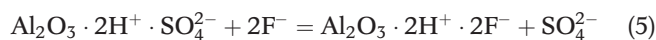
Element	AA	H <sub>2</sub> SO <sub>4</sub> + FeCl <sub>3</sub> -MAA	After adsorption by H <sub>2</sub> SO <sub>4</sub> + FeCl <sub>3</sub> -MAA
Al	50.74	50.19	50.07
O	48.64	48.78	48.52
F	0.20	0.25	0.60
Si	0.18	0.13	0.13
S	0.12	0.47	0.28
Ca	0.04	0.02	0.02
Fe	0.02	0.07	0.06
Ga	0.03	0.03	0.03
Na	0.03	ND	ND
Cl	ND	0.07	0.02

ND: not detected.

**Table 5** | Anionic concentrations in water of different adsorbents after adsorption

Adsorbents	Initial fluoride concentration (mg/L)	F <sup>-</sup> (mg/L)	Cl <sup>-</sup> (mg/L)	SO <sub>4</sub> <sup>2-</sup> (mg/L)
AA	0	0.02	0.64	1.14
	5	1.64	0.63	5.21
	20	14.27	0.72	6.98
H <sub>2</sub> SO <sub>4</sub> + FeCl <sub>3</sub> -MAA	0	0.01	5.42	0.60
	5	0.37	6.69	7.22
	20	5.62	6.80	20.37

and FeCl<sub>3</sub>. Moreover, the concentration of SO<sub>4</sub><sup>2-</sup> ions increased with increasing initial fluoride concentration. Therefore, the significant increase in the adsorption capacity of H<sub>2</sub>SO<sub>4</sub> + FeCl<sub>3</sub>-MAA may be attributable to ion-exchange between SO<sub>4</sub><sup>2-</sup> and F<sup>-</sup> ions. In aqueous solution, H<sup>+</sup>, Al<sup>3+</sup> and Fe<sup>3+</sup> ions were adsorbed on adsorbents. SO<sub>4</sub><sup>2-</sup> ions were adsorbed on the surface of H<sub>2</sub>SO<sub>4</sub> + FeCl<sub>3</sub>-MAA because of electrostatic interaction, and further exchanged with F<sup>-</sup> ions during defluoridation. The possible reaction mechanism for adsorption of fluoride onto H<sub>2</sub>SO<sub>4</sub> + FeCl<sub>3</sub>-MAA can be hypothesized as follows:



## CONCLUSIONS

1. The adsorption capacities of H<sub>2</sub>SO<sub>4</sub>-MAA, FeCl<sub>3</sub>-MAA, and H<sub>2</sub>SO<sub>4</sub> + FeCl<sub>3</sub>-MAA were obviously higher than AA. The adsorption capacity increased quickly at first and then a slow increase was observed until equilibrium was reached. The fluoride content in water adsorbed by MAA was below the standards for drinking water quality in China when the initial concentration of fluoride is 5 mg/L. The equilibrium time of MAA was 8 hours at

low initial fluoride and 12 hours at high initial fluoride. The observed kinetics behavior of the three samples of MAA can be better approximated by pseudo-second-order kinetics. The adsorption process of MAA was better fitted by the Langmuir adsorption isotherm. The maximum adsorption capacity of H<sub>2</sub>SO<sub>4</sub> + FeCl<sub>3</sub>-MAA (4.98 mg/g) was 3.4 times that of AA. The adsorption process of MAA was better fitted by the Langmuir adsorption isotherm.

2. According to the results of BET, the surface area of H<sub>2</sub>SO<sub>4</sub>-MAA was higher than AA because of impurities in pores dissolved by H<sub>2</sub>SO<sub>4</sub>. The result of XRF and ICP showed that the adsorption capacity of H<sub>2</sub>SO<sub>4</sub> + FeCl<sub>3</sub>-MAA significantly increased through ion-exchange between SO<sub>4</sub><sup>2-</sup> and F<sup>-</sup> ions.

## ACKNOWLEDGMENT

This study was supported by the National High Technology Research and Development Program of China (No. 2012AA062605).

## REFERENCES

- Ayoob, S. & Gupta, A. K. 2007 Sorptive response profile of an adsorbent in the defluoridation of drinking water. *Chem. Eng. J.* **133**, 273–281.
- Bang, S., Korfiatis, G. P. & Meng, X. G. 2005 Removal of arsenic from water by zero-valent iron. *J. Hazard. Mater.* **121**, 61–67.
- Bhatnagar, A., Kumar, E. & Sillanpaa, M. 2011 Fluoride removal from water by adsorption – A review. *Chem. Eng. J.* **171**, 811–840.
- Camacho, L. M., Torres, A., Saha, D. & Deng, S. G. 2010 Adsorption equilibrium and kinetics of fluoride on sol-gel-derived activated alumina adsorbents. *J. Colloid. Interf. Sci.* **349**, 307–313.
- Daifullah, A. A. M., Yakout, S. M. & Elreefy, S. A. 2007 Adsorption of fluoride in aqueous solutions using KMnO<sub>4</sub>-modified activated carbon derived from steam pyrolysis of rice straw. *J. Hazard. Mater.* **147**, 633–643.
- Ghorai, S. & Pant, K. K. 2004 Investigations on the column performance of fluoride adsorption by activated alumina in a fixed-bed. *Chem. Eng. J.* **98**, 165–173.
- Ghorai, S. & Pant, K. K. 2005 Equilibrium, kinetics and breakthrough studies for adsorption of fluoride on activated alumina. *Sep. Purif. Technol.* **42**, 265–271.

- Ghosh, D., Medhi, C. R. & Purkait, M. K. 2008 Treatment of fluoride containing drinking water by electrocoagulation using monopolar and bipolar electrode connections. *Chemosphere* **73**, 1393–1400.
- Ma, W., Ya, F. Q., Han, M. & Wang, R. 2007 Characteristics of equilibrium, kinetics studies for adsorption of fluoride on magnetic-chitosan particle. *J. Hazard. Mater.* **143**, 96–302.
- Maliyekkal, S. M., Shukla, S., Philip, L. & Nambi, I. M. 2008 Enhanced fluoride removal from drinking water by magnesia-amended activated alumina granules. *Chem. Eng. J.* **140**, 183–192.
- Meenakshi & Maheshwari, R. C. 2006 Fluoride in drinking water and its removal. *J. Hazard. Mater.* **137**, 456–463.
- Meenakshi, S., Sundaram, C. S. & Sukumar, R. 2008 Enhanced fluoride sorption by mechanochemically activated kaolinites. *J. Hazard. Mater.* **153**, 164–172.
- Mohapatra, M., Anand, S., Mishra, B. K., Giles, D. E. & Singh, P. 2009 Review of fluoride removal from drinking water. *J. Environ. Manage.* **91**, 67–77.
- Onyango, M. S., Kojima, Y., Aoyi, O., Bernardo, E. C. & Matsuda, H. 2004 Adsorption equilibrium modeling and solution chemistry dependence of fluoride removal from water by trivalent-cation-exchanged zeolite F-9. *J. Colloid Interface Sci.* **279**, 341–350.
- Sehn, P. 2008 Fluoride removal with extra low energy reverse osmosis membranes: three years of large scale experience in Finland. *Desalination* **223**, 73–84.
- Sivasankar, V., Ramachandramoorthy, T. & Darchen, A. 2011 Manganese dioxide improves the efficiency of earthenware in fluoride removal from drinking water. *Desalination* **272**, 179–186.
- Tavakoli, H. & Ghasemi, M. R. 2010 Equilibrium, kinetics and break through studies for adsorption of hydrogen fluoride on sodium fluoride. *Chem. Eng. Process.* **49**, 435–440.
- Tripathy, S. S. & Raichur, A. M. 2008 Abatement of fluoride from water using manganese dioxide-coated activated alumina. *J. Hazard. Mater.* **153**, 1043–1051.
- Tripathy, S. S., Bersillon, J. L. & Gopal, K. 2006 Removal of fluoride from drinking water by adsorption onto alum-impregnated activated alumina. *Sep. Purif. Technol.* **50**, 310–317.
- Vaaramaa, K. & Lehto, J. 2003 Removal of metals and anions from drinking water by ion exchange. *Desalination* **155**, 157–170.
- WHO 2006 *Guidelines for Drinking-water Quality*, vol. 1, 3rd edition, incorporating first and second addenda. World Health Organization, Geneva.
- Zhang, G. K., He, Z. L. & Xu, W. 2012 A low-cost and high efficient zirconium-modified-Na- attapulgite adsorbent for fluoride removal from aqueous solutions. *Chem. Eng. J.* **183**, 315–324.

First received 7 December 2013; accepted in revised form 15 April 2014. Available online 13 May 2014